Halina ABRAMCZYK, Monika KOPEĆ
LODZ UNIVERSITY OF TECHNOLOGY, LABORATORY OF LASER MOLECULAR SPECTROSCOPY
15 Wróblewskiego St., 93-590 Lodz, Poland

Applications of Raman scattering in biomedicine, telecommunication and thermometry

Abstract

The paper presents a brief review of methodologies and applications based on the spontaneous and stimulated Raman scattering in telecommunication, thermography and biomedicine. We present the results on cancer biodiagnostics by Raman imaging based on the spontaneous Raman scattering. We showed that combined Raman imaging based on spontaneous Raman scattering and AFM are capable of monitoring biomechanics of tumor vascularity, which is markedly heterogeneous with densely vascularized areas supplying oxygen and nutrients to rapidly growing parts of the tumor. The experimental evidence provides greater understanding of the biomechanics of cancer cell and tissue deformability and its interactions with the extracellular matrix environments offering enormous potential for significant new developments in cancer diagnostics, therapy and drug treatment.

Keywords: linear and nonlinear Raman spectroscopy, Raman imaging, cancer, biodiagnostics.

1. Introduction

For many years the linear and nonlinear phenomena of Raman scattering were the matter of concern for relatively narrow circle of professionals dealing with the laser spectroscopy. So far, Raman scattering phenomena have widely been used in chemistry, materials engineering, and physics for research on the nature of interactions, chemical bonds and properties of semiconductors. During the last decade the interest in the spontaneous and stimulated Raman scattering and other nonlinear optical phenomena has significantly increased with the development of optical telecommunication, thermography, and medical imaging. To illustrate this development of Raman scattering in optoelectronics is Raman amplification in optical fiber technology. After 2000, almost all systems (long-haul – defined as ~ 300 to ~ 800 km and ultra-long-haul – above 800 km) have been using Raman amplification, substituting the most conventional in nineties EDFAs, erbium-doped fibre amplifiers. Despite the Raman amplification phenomenon had been demonstrated in optical waveguides by Stolen and Ippen in the beginning of seventies [1], the eighties and the former half of nineties were dominated by EDFA amplifiers. In the latter half of nineties the increase of interest in Raman amplifiers occurred.

Evidently, the physics of Raman scattering phenomenon has remained the same since Raman and Krishnan publication in Nature in 1929 [2]. Raman scattering is inelastic scattering, and measuring the difference between the energy of the incident photons and scattered photons one can obtain the information about vibrations. The energy of the scattered photon can be shifted to lower frequencies (Stokes component) when the incident photon gives part of its energy to the environment bath (mainly vibrations) or to higher frequencies (anti-Stokes component) when the incident photon gets the energy from the bath.

Raman scattering processes can be expressed by the following equation

$$P_i = \chi_{ij}^{(1)} E + \chi_{ijk}^{(2)} E_j E_k + \chi_{ijkl}^{(3)} E_j E_k E_l \qquad (1)$$

where P is the medium's polarization, E is the electric field intensity, $\chi_{ij}^{(1)}$, $\chi_{ijk}^{(2)}$, $\chi_{ijkl}^{(3)}$ are the electric susceptibilities. The first term of the equation refers to the linear polarization and depicts the spontaneous linear Raman scattering. The second term expresses the spontaneous nonlinear Raman scattering (hyperRaman scattering, HRS). The third term corresponds to the stimulated Raman scattering. Raman scattering contains two components: Stokes and anti-Stokes created as a result of Raman light scattering, Stokes component is characterized by smaller energies than the incident photons because part of the photon energy is given to the vibrational degrees of freedom. In contrast, the anti-Stokes component is characterized by higher energies than the incident photons because part of the vibrational energy is given to the scattered photons. The Stokes component has a frequency $\omega_S = \omega_0 - \omega_{vib}$, shifted by the frequency of the vibration mode ω_{vib} of material from which the fiber is built. The anti-Stokes component has a frequency $\omega_S = \omega_0 + \omega_{vib}$, shifted by the frequency of the vibration mode ω_{vib} of material from which the fiber is built. For the glass fiber ω_{vib} is about 440 cm^{-1} (13.2 THz) and it corresponds to the vibrational mode of silica SiO_2. When the power of the pumping laser is sufficiently large and exceeds the threshold value the Raman scattering becomes the stimulated Raman scattering (SRS).

However, for the Raman scattering to be applied there has to occur the significant progress in the optical waveguide technologies [3-5] such as development of low dispersion fibers, in comparison with the standard single-mode fibers (SMF) the amplification grows up to 10 times, development of large power transmitters, development of fiber components such as the diffractive grating, couplers, multiplexers etc.

There are several important applications of the spontaneous Raman scattering. First, the spontaneous Raman scattering is used in Optical Time Domain Reflectometry (OTDR) or Optical Frequency Domain Reflectometry (OFDR) [6-9]. The reflectometer OTDR (optical time domain reflectometer), which is the basic device for controlling the optical line, both before the operation starts and during the operation for periodical checking, is usually based on the phenomenon of light scattering called the Rayleigh scattering or the inelastic Brillouin scattering, related to generation of acoustic wave at frequency f_B. The signal resulting from the Brillouin scattering, with a frequency red-shifted by f_B, propagates backward along the examined optical fiber. The frequency value depends on the optical fiber properties, stresses in the core, temperature. Typical values are of the order of 13 GHz for 1310 nm and 11 GHz for 1550 nm. The same idea of reflectometry can be applied for OTDR or OFDR devices based on the phenomenon of Raman scattering. The analysis of the ratio of Stokes and anti-Stokes intensities in the fiber provide information about temperature. This effect gains more and more interest in several applications in remote temperature sensors.

The second important application of the spontaneous Raman scattering is Raman imaging. Raman microscopy has many advantages over fluorescence microscopy. First of all, Raman spectroscopy needs no external labelling, and uses the induced polarizability (polarizability tensor derivative with respect to the normal coordinates) as a contrast in producing the image. The polarizability produces the vibrational spectra. Thus, the label-free Raman images rely on the contrast provided by the different vibrational spectra in various regions of the biological tissue. Secondly, biochemical signatures of the molecules are much richer as each component of the tissue provides its own pattern of vibrational behavior. For example, nucleic acids, lipids, biological chromophores, proteins are characterized by vibrational peaks in different spectral regions. *Raman spectroscopy* is a novel technique for laboratory research into the biochemistry of *breast cancer*, brain cancer, colon cancer and has potential as an optical biopsy [10-13].

Raman scattering can be observed microscopically using instrumentation very similar to the laser fluorescence microscopy (Fig. 1). The new generation of Raman microscope can offer a powerful non-destructive and non-contact method of sample analysis. One of the greatest benefits is the use of a confocal Raman microscope design. This enables a very small sample area or volume to be analyzed – down to the micron scale. Combining this micro Raman analysis with automated focusing, XYZ movement, makes possible to produce 'chemical' images of a sample with resolution of localization, and distribution as never before. It has become one of the most powerful optical techniques. To create Raman images the following steps have to be implemented:

- microscope has to be coupled to the Raman spectrometer,
- Raman spectra of spatially resolved points have to be collected by a raster-scanning of the focused laser beam over the sample, or by moving the sample through the laser focus in a raster pattern via a high resolution microscope stage. The resulting datasets of 10,000 to 20,000 individual spectra can be converted into spectral images, spectral images have to be improved with different statistical methods, such as Principal Component analysis (PCA), Vertex Component Analysis (VCA), Hierarchical Cluster Analysis (HCA).

In this paper, we present how the methodologies based on spontaneous Raman scattering can revolutionize biomedical diagnostics and therapy of cancer.

2. Methodology: Raman imaging

The Raman microscope (an alpha 300 RSA+ (WITec, Ulm, Germany) model) was equipped with an Olympus microscope coupled via the fiber of a 50 µm core diameter with a spectrometer UHTS (Ultra High Throughput Spectrometer) and a CCD Camera (Andor Newton DU970N-UVB-353) operating in standard mode with 1600×200 pixels at –60°C with full vertical binning. The incident laser beam (doubled SHG of the Nd:YAG laser (532 nm)) of alpha 300 RSA+ was focused on the sample through a 40× dry objective (Nikon, objective type CFI Plan Fluor C ELWD DIC-M, numerical aperture (NA) of 0.60, and a 3.6–2.8 mm working distance) to the spot of 200 nm. The average laser excitation power was 40 mW, with an integration time of 0.2 s. Rayleigh scattered light was removed using an edge filter.

Spectra were collected at one acquisition per pixel and a 600 lines/mm diffraction grating. Prior to the basis analysis, each spectrum was processed to remove cosmic rays, increase the signal-to-noise ratio via spectral smoothing (Savitzky-Golay method), subtract a signal arising from the (CaF_2) substrate and correct for biological autofluorescence. The large number of spectra collected in this study required the use of automated removal method for all of the spectra, which is critical to remove sources of variability arising from autofluorescence and substrate contamination. After baseline removal, the dominant remaining source of distinction between spectra is the intensity of the Raman features, arising from the variable amount of biological material within the sample. Data acquisition and processing was performed using WITec Project 4.1. The 2D array images of tens of thousands of individual Raman spectra were evaluated by the cluster analysis and basis analysis method (BAM). In BAM method, each measured spectrum of the 2D spectral array is compared to basis spectra using a least squares fit. Such basis spectra are created as the average spectra from different areas in the sample. The weight factor at each point is represented as a 2D image of the corresponding colour and mixed colouring component. The colour code of Raman maps were based on the integrated Raman intensities in specific regions (sum option in the filter manager in the Witec project 4.1). Using a lookup table, bright colors indicate the highest intensities, whereas dark colours indicate the lowest intensities of the chosen region [10-13].

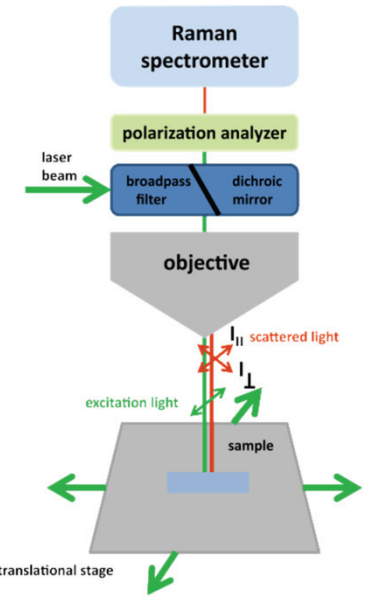

Fig. 1. The configuration of the polarized Raman imaging (PRI) with alpha 300 RSA+ (WITec, Ulm, Germany)

3. Results

Biochemical composition and stiffness measurements of tumor tissue show unique correlation with strong epidemiological data indicating a role for increased mammographic density (MD) in predisposing to breast cancer. A combination of AFM and Raman confocal microscopy will allow connecting mechanical parameters (stiffness, adhesion) with biochemical composition of the tissue. The main beneficial feature of this combination is better understanding of biochemical reasons for the nanomechanical observed differences at the cell and tissue levels during cancer development. We looked inside human breast ducts by Raman imaging answering questions about location and distribution of various biochemical components inside the lumen, epithelial cells of the duct and the stroma around the duct during cancer development [13]. This kind of spatial information by monitoring various chemical constituents in defined cellular compartments of the breast tissue has been reported for the first time. Fig. 2 shows distribution of the main constituents of the normal breast tissue corresponding to "margins of resection," referring to the surrounding tissue that is removed along with a breast tumor. Fig. 2 shows the heterogeneous distribution of biochemical species in a negative margin where no cancer cells are found. Figure 2 shows the white light microscopy image (A), Raman image (B) and the characteristic vibrational Raman spectra (C) corresponding to the specific structures identified by the Raman images. Comparison of Raman image (Fig. 2B) with the white light microscopy image (Fig. 2A) shows that we were able to develop a proper tool for biomedical analysis to get an excellent reproducibility of tissue structures. However, Raman images provides much more than the morphology, it delivers information about the biochemical composition of the tissue. One can see that it is dominated by proteins (red), lipids (blue) and glycans (green).

We have also analyzed the Raman images for the tissue from the tumor mass and the results clearly demonstrate that the composition of the epithelial cells surrounding the lumen of the cancerous duct changes dramatically in comparison with the normal duct [13]. In the view of the results obtained from the Raman imaging we have concentrated on the nanomechanical signature of breast cancer. We have measured the stiffness of the normal and cancerous human breast tissue by AFM method. The elasticity measurements have been performed using atomic force microscope working in a spectroscopy mode AFM AC. The Young's modulus was calculated, taking into account all values

obtained from a set of force versus indentation curves. Detailed information is available in the paper [10]. The results showed that the cancer tissues are characterized by larger Young's modulus value.

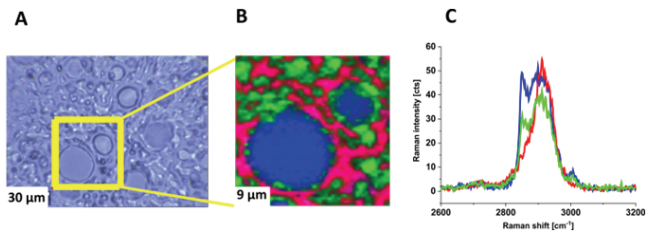

Fig. 2. Distribution of the proteins (red), glycans (green) and lipids (blue) in the human breast normal tissue, the white light microscopy image (A), Raman image (35×35 µm) obtained from the basis analysis in the high frequency spectral region (C) (Patient P157, WHO G2), integration time for Raman images 0.5 s in the high frequency region and 1s in the low frequency region, resolution step 1 um, laser excitation power 10 mW. The line colours of the spectra correspond to the colours of the Raman maps

4. Conclusions

The main beneficial features of Raman phenomenon both the spontaneous and stimulated Raman scattering can be summarized as follows: Raman gain takes place in every fiber, which permits to avoid the expensive material modifications, the gain is non-resonant, so it can be employed in the whole range of light penetrability in fibers that is from 300 nm to 2000 nm. The main Raman application in the linear range covers Optical Time Domain Reflectometry (OTDR) or Optical Frequency Domain Reflectometry (OFDR), remote temperature sensors, and Raman imaging. The nonlinear range covers Raman amplifiers in telecommunication. We have shown that Raman imaging provides a tool for better understanding of biochemical reasons for the nanomechanical properties and biological mechanisms at the cell and tissue levels during cancer development. Oncogenically transformed cells are expected to have differences in all cell and tissue layers, but it still remains unclear whether a mechanical (stiffness, adhesion) or biochemical alterations are a cause or a consequence of cancer development. Biomechanical imaging by Raman/AFM will help to obtain a more reliable diagnosis that begins at present with mammography imaging and histological staining.

This work was supported by the National Science Center of Poland (grant UMO-2015/19/B/ST4/01878, Dz. St. 2017.

5. References

[1] Stolen R. H., Ippen E. P.: Raman gain in glass optical waveguides. Applied Physics Letters, vol. 22, issue 6, pp. 276-278, 1973.
[2] Raman C. V., Krishnan K. S.: A new type of secondary radiation. Nature, vol. 121, pp. 501-502, 1928.
[3] Hecht J.: Raman amplifiers boost system margins at high speed. Laser Focus World, vol. 37, no. 6, pp. 135-140, 2001.
[4] Hecht J.: Mitigating nonlinear effects is essential to long-haul transmission systems, Laser Focus World, vol. 38, no. 5, pp. 155-162, 2002.
[5] Islam M., Nietubyc M.: Not a pretty picture. WDM solutions 3(3), March 2001.
[6] Williams G. R., Brown G., Hawthorne W., Hartog A. H., Waite P. C.: Distributed temperature sensing (DTS) to characterize the performance of producing oil wells. Proc. Int. Society for Optical Engineering (SPIE), vol. 4202, pp. 39–54, 2000.
[7] Guo J., Xia T., Zhang R., Li X.: A novel multimode fiber for distributed temperature sensing based on anti-stokes Raman scattering. Photonics Global Conference (PGC), 2012.
[8] Hausner M. B., Suárez F., Glander K. E., van de Giesen N., Selker J. S., Tyler S. W.: Calibrating Single-Ended Fiber-Optic Raman Spectra Distributed Temperature Sensing Data. Sensors, vol. 11, pp. 10859 – 10879, 2011.
[9] van de Giesen N., Steele-Dunne S. C., Jansen J., Hoes O., Hausner M. B., Tyler S., Selker J.: Double-Ended Calibration of Fiber-Optic Raman Spectra Distributed Temperature Sensing Data. Sensors, vol. 12, pp. 5471-5485, 2012.
[10] Abramczyk H., Imiela A.: The biochemical, nanomechanical and chemometric signatures of brain cancer. Spectrochimica Acta Part A: Molecular and Biomolecular Spectroscopy, accepted for publication.
[11] Imiela A., Polis B., Polis L., Abramczyk H.: Novel strategies of Raman imaging for brain tumor research, Oncotarget, 2017, accepted for publication.
[12] Abramczyk H., Surmacki J., Kopeć M., Olejnik A.K., Kaufman-Szymczyk A., Fabianowska-Majewska K.: Epigenetic changes in cancer by Raman imaging, fluorescence imaging, AFM and scanning near-field optical (SNOM). Acetylation in normal and human cancer breast cells MCF10A, MCF7 and MDA-MB-231. Analyst, 2016, DOI: 10.1039/C6AN00859C.
[13] Abramczyk H., Brożek-Płuska B.: New look inside human breast ducts with Raman imaging. Raman candidates as diagnostic markers for breast cancer prognosis: mammaglobin, palmitic acid and sphingomyelin. Analytica Chimica Acta, vol. 909, pp. 91-100, 2016.

Received: 17.10.2016 Paper reviewed Accepted: 05.01.2017

Prof. Halina ABRAMCZYK, DSc

Professor at the Lodz University of Technology (TUL) in Lodz, Poland, MSc degree in physics from the University of Lodz and PhD degree in physical chemistry from TUL, postdoctoral stay at the University of Bielefeld, Germany, habilitation in molecular and laser spectroscopy at TUL, head of the Laboratory of Laser Molecular Spectroscopy of TUL, 2007−2009 Marie Curie Excellence Chair at Max-Born Institute, Berlin. Her research interests are focused on molecular spectroscopy, and applications of Raman spectroscopy and imaging in cancer diagnostics.

e-mail: halina.abramczyk@p.lodz.pl

Monika KOPEĆ, MSc

Monika Kopeć is PhD student in the Institute of Applied Radiation Chemistry, Laboratory of Laser Molecular Spectroscopy at the TUL in Lodz, Poland. She received her Master of Science degree in medical chemistry in 2013 from Lodz University of Technology and Master of Science degree in logistics in 2014 from University of Lodz. She graduated post-graduated studies in forensic biology in 2016 at the University of Lodz. Her research interests are focused on molecular spectroscopy, and applications of Raman spectroscopy and imaging in cancer diagnostics.

e-mail: monika.kopec@p.lodz.pl